nature neuroscience

Unbalanced excitability underlies offline reactivation of behaviorally activated neurons

Mika Mizunuma[1], Hiroaki Norimoto[1], Kentaro Tao[1], Takahiro Egawa[2], Kenjiro Hanaoka[2], Tetsuya Sakaguchi[1], Hiroyuki Hioki[3], Takeshi Kaneko[3], Shun Yamaguchi[4,5], Tetsuo Nagano[2], Norio Matsuki[1] & Yuji Ikegaya[1,6]

Hippocampal sharp waves (SWs)/ripples represent the reactivation of neurons involved in recently acquired memory and are crucial for memory consolidation. By labeling active cells with fluorescent protein under the control of an immediate-early gene promoter, we found that neurons that had been activated while mice explored a novel environment were preferentially reactivated during spontaneous SWs in hippocampal slices *in vitro*. During SWs, the reactivated neurons received strong excitatory synaptic inputs as opposed to a globally tuned network balance between excitation and inhibition.

Pyramidal neurons in the rodent hippocampus often modulate their spiking behaviors depending on the location through which the animal passes. This 'place cell' activity pattern subsequently reappears during SWs/ripples[1,2], which are transient high-frequency field oscillations that spontaneously occur during slow-wave sleep and quiet wakefulness. Such offline reactivation of the animal's experience is crucial for consolidation of memory and working memory[3]. However, several key issues remain unresolved, including (i) how neurons involved in memory are tagged until the memory's retrieval, (ii) how these neurons are selected for reactivation during SWs, and (iii) whether this specific memory retrieval requires external triggers outside the hippocampus. We addressed these questions by devising an *in vitro* assay system that was able to replicate the multineuron activity patterns of the SWs reflecting the previous experiences of the animals.

SWs/ripples spontaneously occurred in the CA1 region of obliquely sliced hippocampal preparations at frequencies of 47 ± 31 events/min (mean ± s.d. of 20 slices; **Supplementary Fig. 1a–c**). They were of CA3 origin (**Supplementary Fig. 1d**). We imaged spike-triggered somatic calcium transients on a Nipkow-disk confocal microscope at 50–200 frames/s from a total of 1,625 neurons in 15 slices that received bulk injections of Oregon Green 488–BAPTA-1AM into the CA1 pyramidal cell layer (**Supplementary Fig. 2a,b** and **Supplementary Movie 1**). The overall rate of calcium transients increased during SWs (**Supplementary Fig. 2c**). An average of 3.5 ± 2.6% of neurons were recruited in a single SW event, whereas 49 ± 34% of neurons were silent throughout our observation periods, which lasted up to 10 min (**Supplementary Fig. 2d**).

We examined whether the pattern of SW activity was associated with an animal's previous experience. Using the promoter for the immediate-early gene *Arc* (also known as *Arg3.1*), we probed active neurons *in vivo* with dVenus, a modified yellow fluorescent protein, in Arc-dVenus transgenic mice[4]. The mice were allowed to freely explore a novel environment. They were killed 120 min later for hippocampal slice preparations (**Supplementary Fig. 3a**). We used two types of environments: an enriched cage, A, and a less-enriched cage, B. In control naive mice, 4.5 ± 0.8% of CA1 neurons expressed dVenus. This ratio increased to 31.4 ± 5.1% and 16.1 ± 5.1% in animals that explored the novel enriched environment A and the novel but less-enriched environment B, respectively, for 30 min, and it further increased to 36.6 ± 4.8% in animals that sequentially explored environments A and B for 15 min each (mean ± s.e.m. of 3 or 4 mice; **Supplementary Fig. 3b,c**). Thus, dVenus expression was correlated with the behavioral experience of the mice.

We prepared slices from animals that had explored the novel environment A for 30 min and loaded the CA1 pyramidal cell layer with CaSiR-1, a near-infrared calcium indicator[5]. In total, we imaged 197 dVenus$^-$ and 90 dVenus$^+$ neurons from 7 slices from 6 mice (**Fig. 1a**). dVenus$^+$ neurons were preferentially activated during SWs relative to dVenus$^-$ neurons (**Fig. 1b**). The preferential SW participation of dVenus$^+$ neurons was also found in slices prepared from naive mice that had not experienced a novel environment (**Supplementary Fig. 4**). Slices from a novel-environment group that were pretreated with zeta inhibitory peptide (ZIP), a peptide that eliminates previously occurring long-term potentiation[6], did not exhibit SWs, nor did the rates of spontaneous calcium transients differ between dVenus$^-$ and dVenus$^+$ neurons (**Fig. 1c**; n = 6 slices from 3 mice). Similarly, the activity rates did not differ in slices pretreated with scrambled ZIP, which is also known to revoke existing long-term potentiation[6] (**Fig. 1c**). The preferential reactivation of dVenus$^+$ neurons was confirmed by targeted whole-cell recordings (**Fig. 1d,e**). Thus, we conclude that *in vitro* SWs are associated with previous behavioral experiences and emerge through ZIP-sensitive synaptic plasticity.

Excitatory and inhibitory postsynaptic currents (EPSCs and IPSCs) were dominant at clamped voltages of −70 and 0 mV (**Fig. 2a**). All neurons, including silent cells, exhibited phasic EPSCs and IPSCs during SWs. The mean time course of the EPSCs during SWs was similar to that of the IPSCs (**Fig. 2b**), although the EPSCs slightly preceded the IPSCs (**Fig. 2c,d**). Thus, the excitation/inhibition (E/I) ratio was largely balanced throughout a SW event.

We separated neurons into silent cells (nonparticipants) and SW-participating cells (participants). The mean peak amplitudes

[1]Laboratory of Chemical Pharmacology, Graduate School of Pharmaceutical Sciences, University of Tokyo, Tokyo, Japan. [2]Laboratory of Chemistry and Biology, Graduate School of Pharmaceutical Sciences, University of Tokyo, Tokyo, Japan. [3]Department of Morphological Brain Science, Graduate School of Medicine, Kyoto University, Kyoto, Japan. [4]Division of Morphological Neuroscience, Gifu University Graduate School of Medicine, Gifu, Japan. [5]PRESTO, Japan Science and Technology Agency, Saitama, Japan. [6]Center for Information and Neural Networks, Suita City, Osaka, Japan. Correspondence should be addressed to Y.I. (ikegaya@mol.f.u-tokyo.ac.jp).

Received 23 December 2013; accepted 6 February 2014; published online 16 March 2014; doi:10.1038/nn.3674

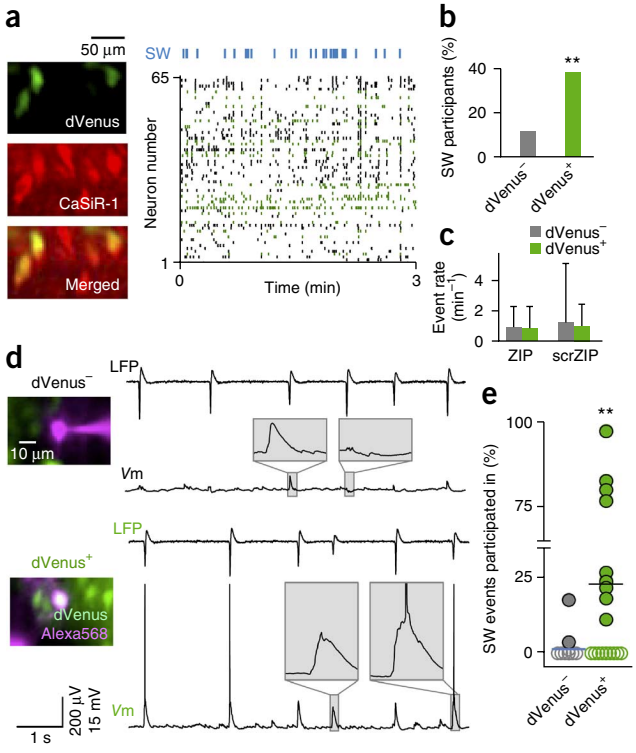

Figure 1 Reactivation of behaviorally activated neurons during *in vitro* SWs. (**a**) Calcium imaging from dVenus⁻ and dVenus⁺ CA1 neurons loaded with CaSiR-1. (**b**) dVenus⁺ neurons participated more frequently in SWs than dVenus⁻ neurons. $^{**}P = 3.6 \times 10^{-7}$, Fisher's exact test, $n = 197$ dVenus⁻ and 90 dVenus⁺ cells. (**c**) Spontaneous activity rates in slices treated with ZIP and scrambled ZIP (scrZIP), peptides known to eliminate previously occurring long-term potentiation, did not differ between dVenus⁻ and dVenus⁺ neurons. $n = 123$ or 115 dVenus⁻ and 75 or 51 dVenus⁺ cells. Error bars are s.d. of 6 slices from 3 mice. (**d**) dVenus⁻ (top) and dVenus⁺ (bottom) neurons were loaded with Alexa Fluor 568 and current-clamped at $I = 0$. (**e**) dVenus⁺ neurons participated more frequently in SWs than dVenus⁻ neurons. $^{**}P = 0.0057$, Mann-Whitney U test, $n = 20$ dVenus⁻ and 19 dVenus⁺ cells in 21 slices from 21 mice.

of the SW-relevant EPSCs (**Fig. 2e**) or IPSCs (**Fig. 2f**) did not differ between the SW nonparticipants and participants; however, the EPSC-to-IPSC ratios of the mean charges were significantly higher in SW participants than nonparticipants (**Fig. 2g** and **Supplementary Table 1**). In contrast, the differences in the peak timings between the EPSCs and IPSCs did not differ between SW participants and nonparticipants (**Fig. 2h**). During the baseline periods without SWs, the mean amplitudes and frequencies of spontaneous EPSCs and IPSCs or their E/I ratios did not differ between SW participants and nonparticipants (**Supplementary Fig. 5** and **Supplementary Table 1**). Moreover, neither the resting membrane potential nor the input resistance differed between nonparticipants and participants (**Supplementary Fig. 6**). Thus, the E/I balance in the SW participants was biased toward excitation during SWs.

To determine whether this unbalanced E/I ratio was causal for SW-locked spiking, we used a dynamic clamp technique and injected combinatorial conductances with SW-relevant EPSC-like and IPSC-like waveforms into CA1 pyramidal cells in the presence of a cocktail of ionotropic glutamate and GABA receptor antagonists (**Supplementary Fig. 7**). Although both the E/I balance and the E/I timing of the injected conductances contributed significantly to the spike probability of the neuron, the E/I balance was a dominant determinant ($F_{6,392} = 153.2$ for balance versus $F_{6,392} = 6.6$ for timing; two-way ANOVA, $n = 9$ cells, 20 trials each).

We examined whether the amplitudes of the SW-relevant EPSCs and IPSCs correlated with the amplitude of SW field potentials. The sizes of the individual EPSCs and IPSCs were standardized as Z-scores in each cell, and the pooled data from 39 cells were plotted against the standardized amplitudes of the corresponding SW events. Both the EPSC and IPSC sizes correlated significantly with the SW size (**Fig. 3a**; $r^2 = 0.15$, $P < 0.001$, $n = 1{,}542$ EPSCs; $r^2 = 0.46$, $P < 0.001$, $n = 1{,}139$ IPSCs), and the IPSC size correlated more tightly than the EPSC size ($P < 10^{-16}$, $Z = 9.38$, Z-test for two correlation coefficients). Thus, the IPSCs are more globally tuned and report summed excitatory inputs from CA3, whereas the EPSCs reflect inputs from more specific CA3 neuron ensembles.

Parvalbumin (PV) is a cellular marker for a subclass of GABAergic interneurons. We patched fast-spiking PV⁺ neurons from PV-GFP transgenic mice (**Fig. 3b,c**)[7]. During SWs, PV⁺ cells reliably emitted single or multiple spikes[8], and the numbers of spikes were nearly linearly related to the SW amplitude (**Fig. 3d**; $n = 10$ cells from 4 slices). In accord with this, PV⁺

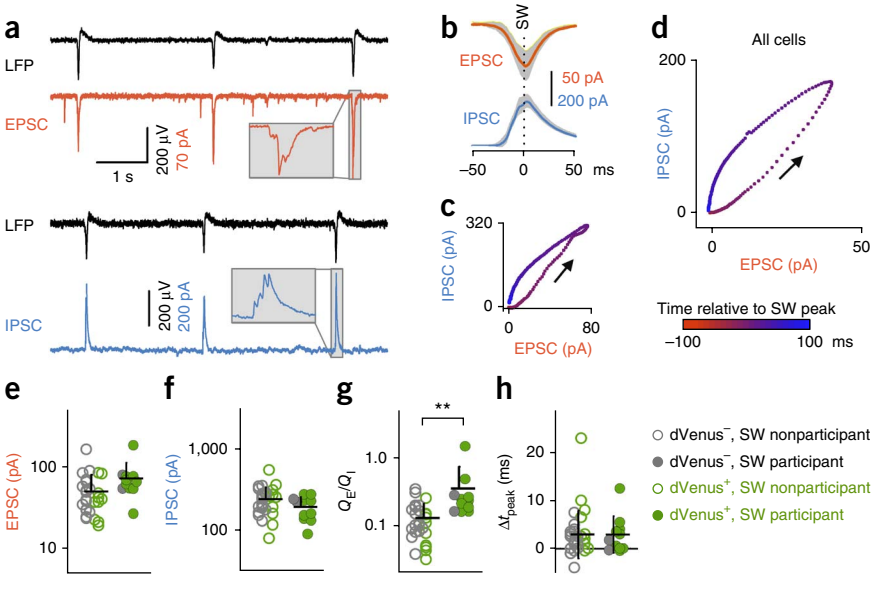

Figure 2 E/I imbalance during SWs. (**a**) EPSCs (top) and IPSCs (bottom) in a CA1 pyramidal cell during SWs. (**b**) Mean ± s.d. of 122 EPSCs (top) and 86 IPSCs (bottom) relative to the SW peak timings in the same neuron as in **a**. All SW-locked EPSCs and IPSCs recorded from this neuron were pooled. (**c**) Time evolution of the mean EPSC and IPSC in **b**. (**d**) The E/I time evolution averaged across all SWs recorded from 39 cells (from 21 slices in 21 mice). (**e**–**h**) The mean peak amplitude of SW-relevant EPSCs (**e**), the mean peak amplitude of SW-relevant IPSCs (**f**), the EPSC-to-IPSC ratio of the mean charge (**g**), and the mean delay between EPSC and IPSC peak timings (**h**), compared between 28 SW nonparticipants and 11 SW participants. Error bars, s.d. The y axes are logarithmic in **e**–**g**. $^{**}P = 0.0008$, $U_{11,28} = 47$, Mann-Whitney-Wilcoxon test.

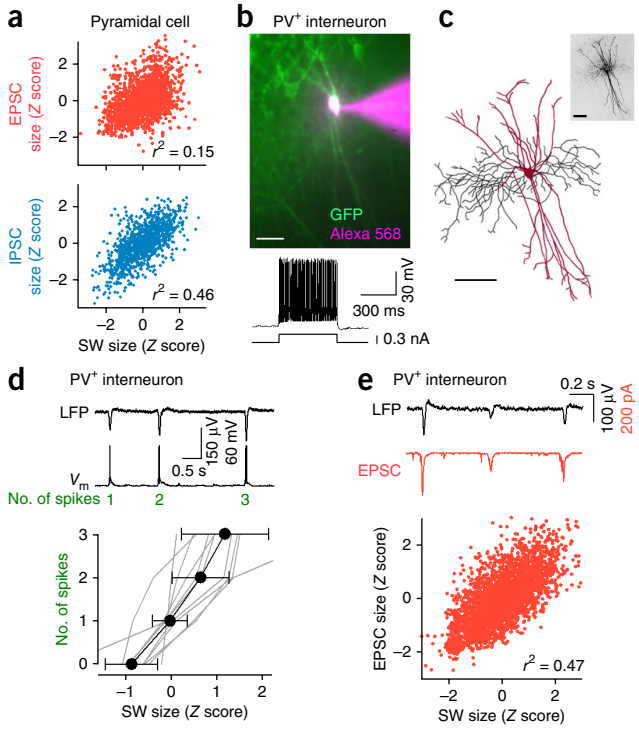

Figure 3 Linearly tuned inhibitory activity. (**a**) SW-relevant EPSC sizes recorded in CA1 pyramidal cells (top) were less correlated than the IPSC sizes (bottom) with the corresponding SW sizes: r^2 = 0.15, n = 1,542 EPSCs; r^2 = 0.46, n = 1,139 IPSCs; from 39 cells (in 21 slices from 21 mice). (**b**) A PV+ interneuron, which exhibited nonadaptive spiking (bottom), was targeted for whole-cell recording (bottom) using Alexa Fluor 568 in a PV-GFP transgenic mouse slice (top). Scale bar, 50 µm. (**c**) A putative PV+ basket cell, reconstructed from a biocytin–Alexa Fluor 594 photograph (inset). Scale bar, 100 µm. (**d**) The number of spikes emitted by PV+ cells during SWs was linear with the SW size. Gray lines indicate individual cells, and the black line represents the means ± s.d. of 2,901 SWs from 10 cells (in 6 slices from 4 mice). (**e**) The sizes of SW-relevant EPSCs recorded in PV+ cells correlated positively with the SW size: r^2 = 0.47, n = 3,032 SWs from 10 cells (in 6 slices from 4 mice).

cells received EPSCs that strongly correlated with SW size, unlike pyramidal cells (**Fig. 3e**; r^2 = 0.47, P < 0.001, n = 3,032 EPSCs).

In this work, we demonstrated that, without extrahippocampal afferents, hippocampal microcircuitry can selectively reactivate behaviorally relevant neurons. This *in vitro* activity retrieval phenomenon allowed us to distinguish experience-related neurons from other neurons and to investigate the synaptic mechanisms underlying neuronal reactivation. We then discovered that in an E/I-balanced network, a few select neurons received stronger EPSCs and were thereby driven to fire action potentials during SWs. Because SW-irrelevant synaptic activity did not differ between SW participants and nonparticipants, excitatory synapses involved in behavioral experience were specifically potentiated; however, whether the responsible synapses are selected by behavioral exploration or are preselected before exploration is yet to be elucidated.

METHODS

Methods and any associated references are available in the online version of the paper.

Note: Any Supplementary Information and Source Data files are available in the online version of the paper.

ACKNOWLEDGMENTS

This work was supported by Grants-in-Aid for Science Research (22115003, 23115101, 25119004 and 25123709; the Japanese Ministry of Education, Culture, Sports, Science and Technology), the Funding Program for Next Generation World-Leading Researchers (LS023; the Japan Society for the Promotion of Science) and the Strategic Research Program for Brain Sciences.

AUTHOR CONTRIBUTIONS

M.M. and Y.I. designed the study. M.M., H.N. and K.T. conducted the experiments. M.M., H.N., K.T., T.S. and Y.I. analyzed the data. T.E., K.H. and T.N. prepared calcium indicator. H.H., T.K. and S.Y. prepared transgenic mice. M.M. and Y.I. wrote the paper. The study was managed by Y.I. and N.M.

COMPETING FINANCIAL INTERESTS

The authors declare no competing financial interests.

1. Lee, A.K. & Wilson, M.A. *Neuron* **36**, 1183–1194 (2002).
2. Wilson, M.A. & McNaughton, B.L. *Science* **265**, 676–679 (1994).
3. Girardeau, G., Benchenane, K., Wiener, S.I., Buzsaki, G. & Zugaro, M.B. *Nat. Neurosci.* **12**, 1222–1223 (2009).
4. Eguchi, M. & Yamaguchi, S. *Neuroimage* **44**, 1274–1283 (2009).
5. Egawa, T. *et al. J. Am. Chem. Soc.* **133**, 14157–14159 (2011).
6. Volk, L.J., Bachman, J.L., Johnson, R., Yu, Y. & Huganir, R.L. *Nature* **493**, 420–423 (2013).
7. Kameda, H. *et al. Eur. J. Neurosci.* **35**, 838–854 (2012).
8. Hájos, N. *et al. J. Neurosci.* **33**, 11677–11691 (2013).

ONLINE METHODS

Animal ethics. Experiments were performed with the approval of the animal experiment ethics committee at the University of Tokyo (approval numbers 21-6 and 24-8) and according to the University of Tokyo guidelines for the care and use of laboratory animals.

Drugs. D,L-2-Amino-5-phosphonopentanoic acid (AP5) and 6-cyano-7-nitroquinoxoxaline-2,3-dione disodium salt (CNQX) were dissolved to 10 mM in water and stored at 4 °C. Immediately before use, AP5 and CNQX were diluted to their final concentrations with artificial cerebrospinal fluid (aCSF) containing (in mM) 127 NaCl, 3.5 KCl, 1.24 KH_2PO_4, 1.2 $MgSO_4$, 2.0 $CaCl_2$, 26 $NaHCO_3$, and 10 D-glucose. Picrotoxin, zeta inhibitory peptide (ZIP), and scrambled ZIP were dissolved directly in aCSF before use.

Behavioral procedure. Wild-type or Arc-dVenus transgenic C57BL/6J mice of either sex (4–5 weeks old) were singly housed for 5 d before the experiments. On the experimental day, the mice were placed in a novel rectangular chamber (280 mm wide, 600 mm long, 250 mm high) and were allowed to explore for 30 min. Two types of chambers (A and B) were prepared. Type A was an enriched environment that contained a running wheel, tunnels and three small toys (plastic blocks), whereas type B was less enriched, with only three toys. Animals were randomly assigned to one of these chambers. The mice were subsequently returned to their home cages. After 120 min, acute slices were prepared. For the experiment in **Supplementary Figure 3**, the mice were killed 5 h after exploration.

Slice preparation. Acute slices were prepared from the medial to ventral part of the hippocampal formation. Mice were anesthetized with ether and decapitated, and the brain was horizontally sliced (400 μm thick) at an angle of 12.7° to the fronto-occipital axis using a vibratome and an ice-cold oxygenated cutting solution consisting of (in mM) 222.1 sucrose, 27 $NaHCO_3$, 1.4 NaH_2PO_4, 2.5 KCl, 1 $CaCl_2$, 7 $MgSO_4$, and 0.5 ascorbic acid[9]. This cutting angle preserved more Schaffer collaterals in slices (**Supplementary Fig. 1b,c**). Two to four slices per mouse were usable in the experiments. Slices were allowed to recover for at least 1.5 h submerged in a chamber filled with oxygenated aCSF at room temperature. In some experiments, slices were incubated in aCSF supplemented with 2 μM ZIP and scrambled ZIP for 2 h during this recovery period.

***In vitro* electrophysiology.** Recordings were performed in a submerged chamber perfused at 8 ml/min with oxygenated aCSF at 35–37 °C. Local field potentials (LFPs) were recorded from the CA1 stratum pyramidale or stratum radiatum using borosilicate glass pipettes (1–2 MΩ) filled with aCSF. Whole-cell patch-clamp recordings were obtained from CA1b/c pyramidal cells visually identified under infrared differential interference contrast microscopy. Patch pipettes (3–6 MΩ) were filled with a potassium-based solution consisting of (in mM) 120 potassium gluconate, 10 KCl, 10 HEPES, 10 creatine phosphate, 4 Mg-ATP, 0.3 Na_2-GTP and 0.2 EGTA. Parvalbumin (PV)-containing interneurons were targeted in slices prepared from PV-GFP transgenic mice[7]. To visualize cell morphology, 200 μM Alexa Fluor 568 hydrazide or 0.2% biocytin was added to the intrapipette solution. Spontaneous excitatory and inhibitory postsynaptic currents (EPSCs and IPSCs) were recorded at clamped voltages of −70 and 0 mV, respectively, in the absence of glutamatergic or GABAergic receptor antagonists. The postsynaptic currents recorded at −70 mV were abolished following the addition of 20 μM CNQX and 50 μM AP5, whereas those recorded at 0 mV were abolished by 50 μM picrotoxin. The driving forces for EPSCs at −70 mV and IPSCs at 0 mV were almost equivalent in our extracellular and intracellular solutions. Series resistance was compensated at most by 15%. Once a satisfactory recording was obtained, the input resistance of the neuron was measured by passing a 500-ms current of from −0.1 to −0.02 nA at steps of 0.02 nA. For each neuron, spike responses to a brief inward current were examined. For pyramidal cells, regular spiking neurons were selected for the subsequent analyses. For PV^+ cells, neurons that fired lately in response to a weak threshold current injection were selected because these neurons are more likely basket cells rather than axo-axonic cells[10]. The signal was digitized at 10 kHz and filtered with a band of 1–2,000 Hz. The onset timings of the EPSCs and IPSCs were defined as the time when the currents reached 20% of the peak current amplitudes. Liquid junction potentials were not corrected. Data were analyzed offline using custom-made MATLAB routines. Well-trained investigators blind to the dVenus positivity results analyzed the electrophysiological data.

Optical recording. Functional multineuron calcium imaging was conducted using slices loaded locally with Oregon Green BAPTA-1AM and CaSiR-1AM, both of which can detect single spikes[11]. CaSiR-1AM was chemically synthesized in our laboratory[5]. Oregon Green 488 BAPTA-1AM and CaSiR-1AM were dissolved in DMSO containing 10% Pluronic F-127 to yield a concentration of 200 μM. Immediately before use, this solution was diluted 1:10 with aCSF and loaded into pipettes (3–5 MΩ). The tip of the pipette was inserted into the CA1 stratum pyramidale, and a pressure of 50–60 hPa was applied for 3–5 min using a 10-ml syringe pressurizer. Fluorophores were excited at 488 nm and 633 nm with laser diodes and visualized using 507-nm and 660-nm long-pass emission filters, respectively. Videos were recorded at 50–200 frames/s using a 16× objective, a spinning-disk confocal microscope and a cooled EM-CCD camera. dVenus was excited at 488 nm and visualized using a 520/535-nm band-pass emission filter. The fluorescence change was measured as $(F_t - F_0)/F_0$, where F_t is the fluorescence intensity at time t and F_0 is the fluorescence intensity averaged from −10 s to 10 s relative to t. Using principal component analysis and a support vector machine optimized to calcium imaging, spike-elicited calcium transients were semiautomatically detected with a custom-written program in Visual Basic and were manually inspected by eye[12]. If noise was erroneously detected, it was manually rejected by an independent experienced researcher who was blind to the experiment designs.

SW detection. SWs/ripples were detected by thresholding filtered traces on the basis of the signal-to-noise ratio. LFP traces were band-pass filtered at 2–30 Hz, and SWs were determined at a threshold at 5 times above the s.d. of the baseline noise. The detected events were scrutinized by eye and manually rejected if they were erroneously detected. SWs/ripples with event durations of less than 30 ms were also discarded because these events were typically recording artifacts. Because SWs typically last for approximately 100 ms, we defined SW-relevant activity as activity that occurred within 100 ms before and after the SW peak time by taking imaging frame jitters into consideration (**Supplementary Fig. 2b**). We also defined SW participants as neurons that exhibited SW-relevant activity at frequencies of greater than 0.1 per minute.

Dynamic-clamp stimulation. CA1 pyramidal cells were stimulated with dynamic-clamp conductance injection[13]. The command current $I(t)$ was calculated online as $G_e(t) \times (V(t) - E_{e\_rev}) + G_i(t) \times (V(t) - E_{i\_rev})$, where $G_e(t)$ and $G_i(t)$ are the time-varying conductances, $V(t)$ is the membrane potential at time t, and the reversal potentials E_{e_rev} and E_{i_rev} are 0 mV for excitation and −70 mV for inhibition, respectively. $I(t)$ was delivered into patch-clamped neurons at 10 kHz using a real-time Linux environment. As $G_e(t)$ and $G_i(t)$ templates, we used the averaged EPSC and IPSC waveforms during the period from −100 ms to +100 ms relative to the SW peak time in our voltage-clamp recording. The peak amplitude of $G_e(t)$ ranged from 0.53 to 4 nS, and the peak amplitude of $G_i(t)$ was fixed to 4 nS, which was roughly equal to the mean value recorded during SWs. We injected all possible combinations of $G_e(t)$ and $G_i(t)$ into current-clamped neurons, with peak-time differences of 0–6 ms. During this stimulation, intrinsic fast synaptic transmission was blocked by bath application of an inhibitor mixture containing 20 μM CNQX, 50 μM AP5 and 50 μM picrotoxin.

Biocytin visualization. For the visualization of patch-clamped neurons, the slices were fixed in 4% paraformaldehyde and 0.05% glutaraldehyde at 4 °C overnight, then incubated in 0.2% Triton X-100 at 4 °C overnight, and finally incubated overnight at 4 °C with a streptavidin–Alexa Fluor 594 conjugate (1:500).

Statistics. No statistical methods were used to predetermine sample sizes, but our sample sizes are similar to those reported in previous publications[8,9,14,15].

9. Norimoto, H., Mizunuma, M., Ishikawa, D., Matsuki, N. & Ikegaya, Y. *Brain Res.* **1461**, 1–9 (2012).
10. Woodruff, A., Xu, Q., Anderson, S.A. & Yuste, R. *Front. Neural Circuits* **3**, 15 (2009).
11. Takahashi, N. *et al. Curr. Protoc. Neurosci.* **2**, 14 (2011).
12. Sasaki, T., Takahashi, N., Matsuki, N. & Ikegaya, Y. *J. Neurophysiol.* **100**, 1668–1676 (2008).
13. Takahashi, N., Sasaki, T., Matsumoto, W., Matsuki, N. & Ikegaya, Y. *Proc. Natl. Acad. Sci. USA* **107**, 10244–10249 (2010).
14. Sun, Y., Norimoto, H., Pu, X.P., Matsuki, N. & Ikegaya, Y. *J. Pharmacol. Sci.* **118**, 288–294 (2012).
15. Maier, N. *et al. Neuron* **72**, 137–152 (2011).

doi:10.1038/nn.3674

Unbalanced Excitability Underlies Offline Reactivation of Behaviorally Activated Neurons

Mika Mizunuma, Hiroaki Norimoto, Kentaro Tao, Takahiro Egawa, Kenjiro Hanaoka, Tetsuya Sakaguchi, Hiroyuki Hioki, Takeshi Kaneko, Shun Yamaguchi, Tetsuo Nagano, Norio Matsuki, Yuji Ikegaya

Contents

Nature Neuroscience: doi:10.1038/nn.3674

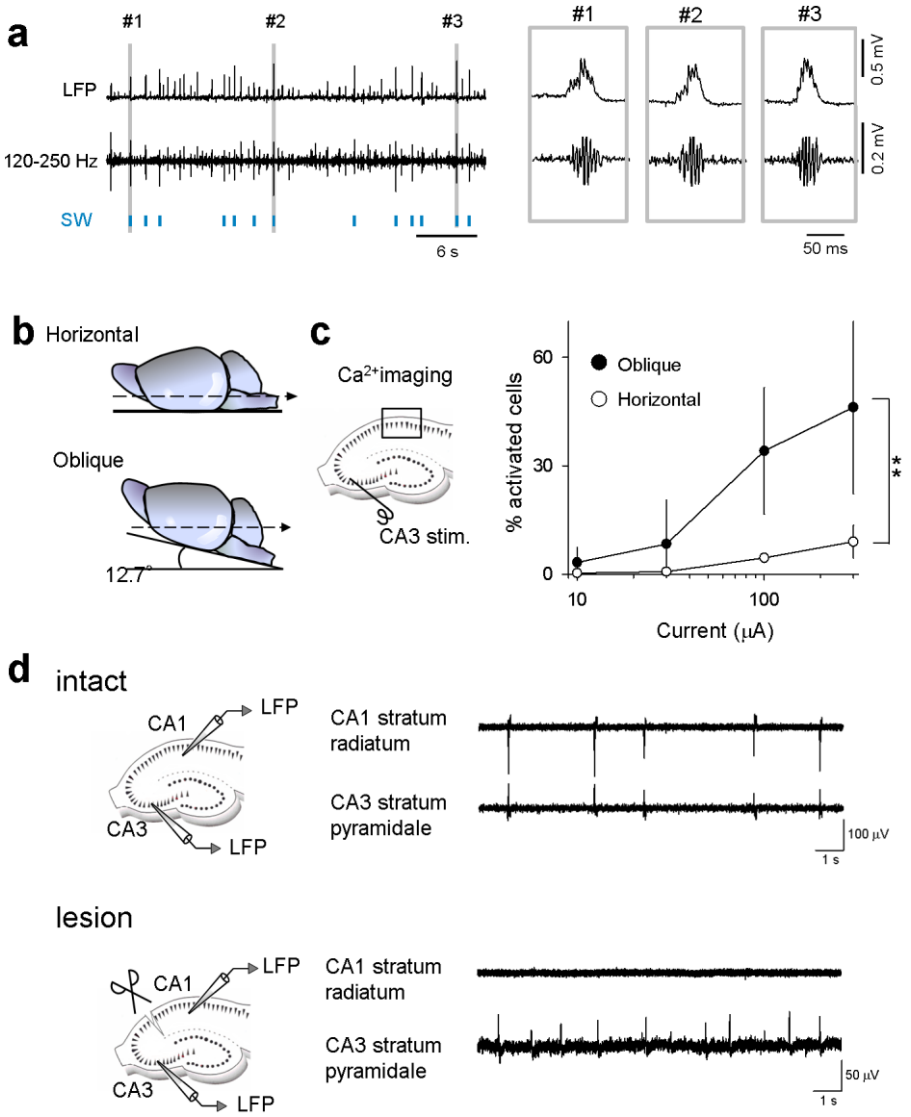

Supplementary Figure 1. SWs *in vitro*. (a) Representative LFP trace (top) and 120–250 Hz filtered trace (bottom) recordings from CA1 stratum pyramidale. SW timings are shown with blue lines. Three SWs are magnified in the left insets. The peak ripple oscillation frequency was 191 ± 22 Hz (mean ± SD). (b) The brains were sliced horizontally (top) or at an angle of 12.7° to the fronto-occipital axis (bottom). (c) CA3 stratum pyramidale was stimulated at various intensities, and neurons that fired in response to the stimulation were monitored in CA1 stratum pyramidale using functional multineuron calcium imaging with Oregon Green 488 BAPTA-1. The mean percentage of spiking neurons to the total neurons recorded in horizontal and oblique slices are plotted as a function of the stimulation intensity. These results imply that CA3-to-CA1 axonal projections were more preserved in oblique slices than in horizontal slices (***P* = 6.6×10^{-5}, $F_{1,28}$ = 21.9, two-way ANOVA). Error bars are SDs of 4 or 5 slices from 3 mice. (d) Paired LFP recordings from CA3 and CA1. SWs in CA1 occurred together with CA3 network activity in an intact hippocampal slice. In slices that received surgical lesions between CA3 and CA1, CA3 network activity still remained, but SWs in CA1 disappeared. (*n* = 3 slices from 2 mice each).

Nature Neuroscience: doi:10.1038/nn.3674

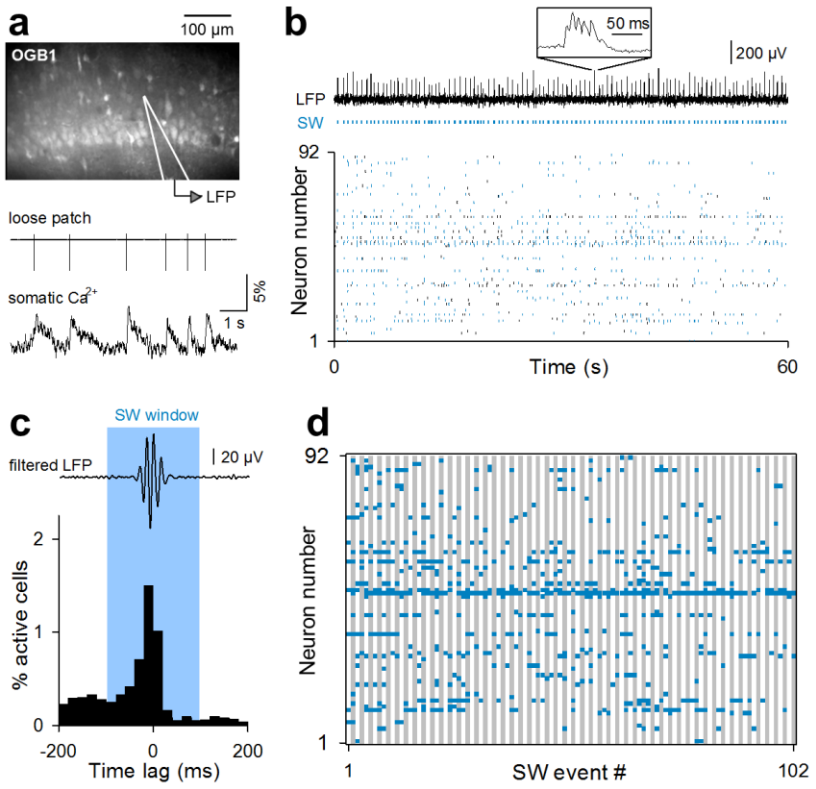

Supplementary Figure 2. Calcium imaging of SW-relevant activities. (a) Functional multineuron calcium imaging from the CA1 stratum pyramidale of an Oregon Green 488 BAPTA-1-loaded slice and recordings of local field potentials (LFP) (top). Simultaneous loose cell-attached recording and calcium imaging (bottom). (b) Representative raster plot of the spiking of CA1 neurons (bottom). SW-relevant activity is shown in blue. SW times (middle) were determined from simultaneously recorded LFPs (top). (c) Peri-SW time histogram of calcium transients (n = 1,625 cells in 15 slices from 15 mice). (d) Neurons activated during each SW event.

Nature Neuroscience: doi:10.1038/nn.3674

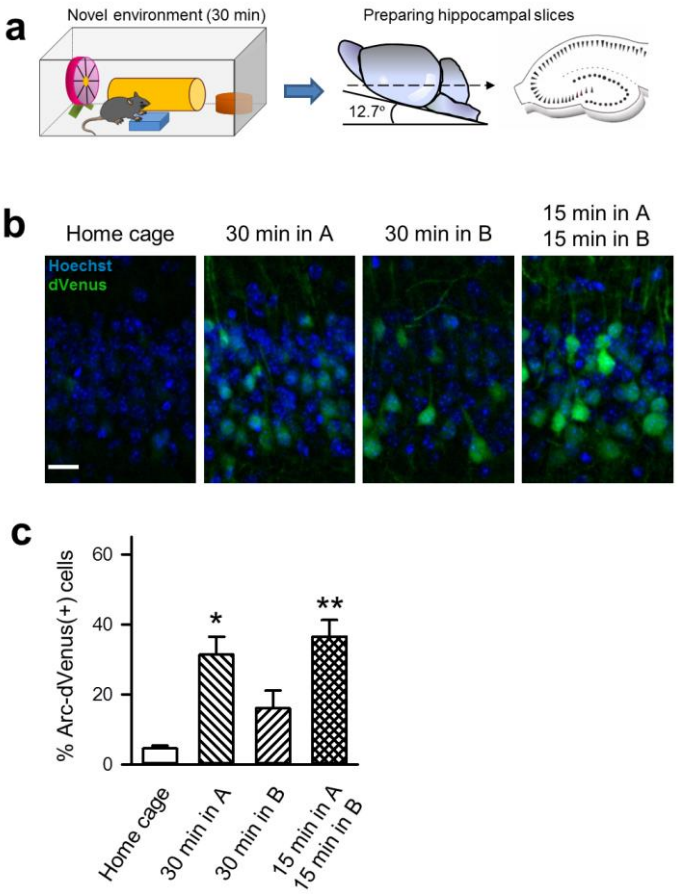

Supplementary Figure 3. dVenus expression after behavioral exploration of Arc-dVenus mice. (a) Schematic illustration of experimental procedures. SWs were monitored in hippocampal slices prepared from Arc-dVenus transgenic mice that had been allowed to explore a novel enriched environment for 30 min. (b) Representative control images of dVenus fluorescence (green) and Hoechst counterstain (blue) in control naïve mice (Home cage), animals that explored the novel enriched environment A for 30 min (30 min in A), animals that explored the novel but less-enriched environment B (30 min in B), and animals that sequentially explored environments A and B for 15 min each (15 min in A/15 min in B). Scale bar = 20 μm. (c) Percentages of dVenus(+) neurons to the total neurons were compared in home-cage mice (n = 3 mice), animals that explored environment A for 30 min (n = 4 mice), animals that explored environment B (30 min in B, n = 4 mice), and animals that explored sequentially explored A and B for 15 min each (15 min in A/15 min in B, n = 3 mice). Three 200-μm-thick sections were prepared per mouse from a middle part (2,600 μm ventral from bregma) of the hippocampus 5 h after the exploration, and 21 confocal sections were taken at a Z interval of 1 μm. Cells were considered dVenus(+) when the mean fluorescence intensity in the soma (ROI Φ = 5 μm) was higher than the background fluorescence intensity by twice its SD. The background intensities were measured from 50 ROIs (Φ = 5 μm) selected randomly from cell body-absent regions in the stratum radiatum in the same histological sections, and their mean and SD were used to detect dVenus(+) neurons. Neurons were identified by their nuclear morphology. Error bars represent the SEM. *P = 0.011, Q = 4.04 *versus* Home cage; **P = 0.0052, Q = 4.50 *versus* Home cage; Tukey's multiple comparison test after one-way ANOVA.

Nature Neuroscience: doi:10.1038/nn.3674

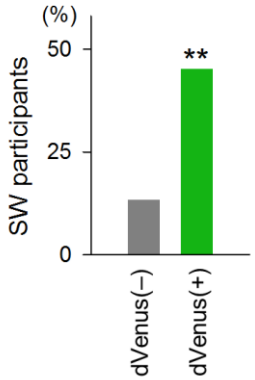

Supplementary Figure 4. Preferential SW participation of dVenus(+) neurons in control mice. dVenus(+) neurons in naïve mice that were not exposed to novel environments were more frequently activated during SWs when compared to dVenus(–) neurons in those mice. $^{**}P = 6.7\times10^{-3}$, Fisher's exact probability test, n = 82 dVenus(–) and 31 dVenus(+) cells in 4 slices in 2 mice.

Nature Neuroscience: doi:10.1038/nn.3674

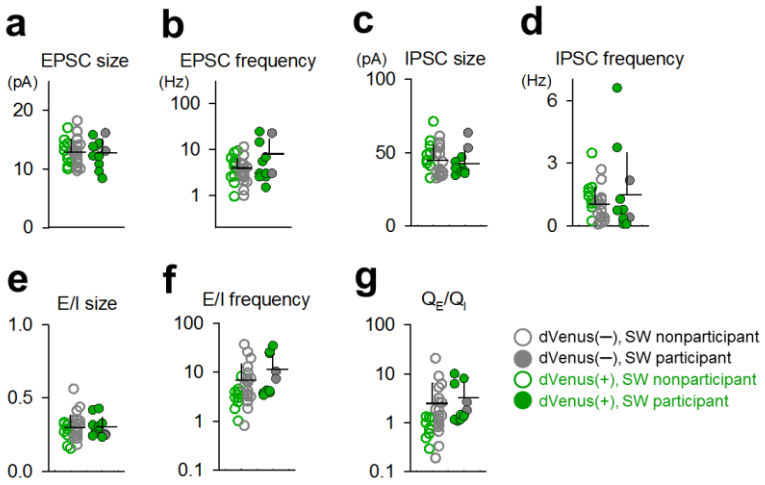

Supplementary Figure 5. No difference in SW-irrelevant, basal synaptic activity between SW participants and nonparticipants. (a-g) The mean sizes (a,c) and frequencies (b,d) of spontaneous EPSCs (a,b) or IPSCs (c,d) and the EPSC-to-IPSC ratio of the mean size (e), the mean frequency (f), and the mean charge (g) during periods without SWs were compared between SW nonparticipants (open circles) and participants (closed circles). Error bars represent the SDs of 28 SW nonparticipants and 11 SW participants. All parameters scored $P > 0.1$, Mann-Whitney-Wilcoxon test.

Nature Neuroscience: doi:10.1038/nn.3674

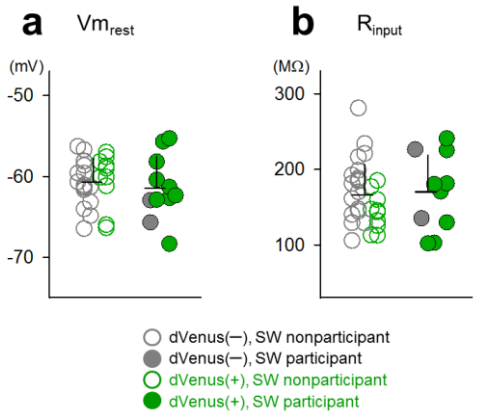

Supplementary Figure 6. No difference in intrinsic properties between SW participants and nonparticipants. (a) Baseline membrane potential (Vm_{rest}) of SW nonparticipants (open circles) and participants (closed circles) is shown. (b) Input resistance (R_{input}) of SW nonparticipants and participants is shown. Error bars represent the SDs of 28 SW nonparticipants and 11 SW participants.

Nature Neuroscience: doi:10.1038/nn.3674

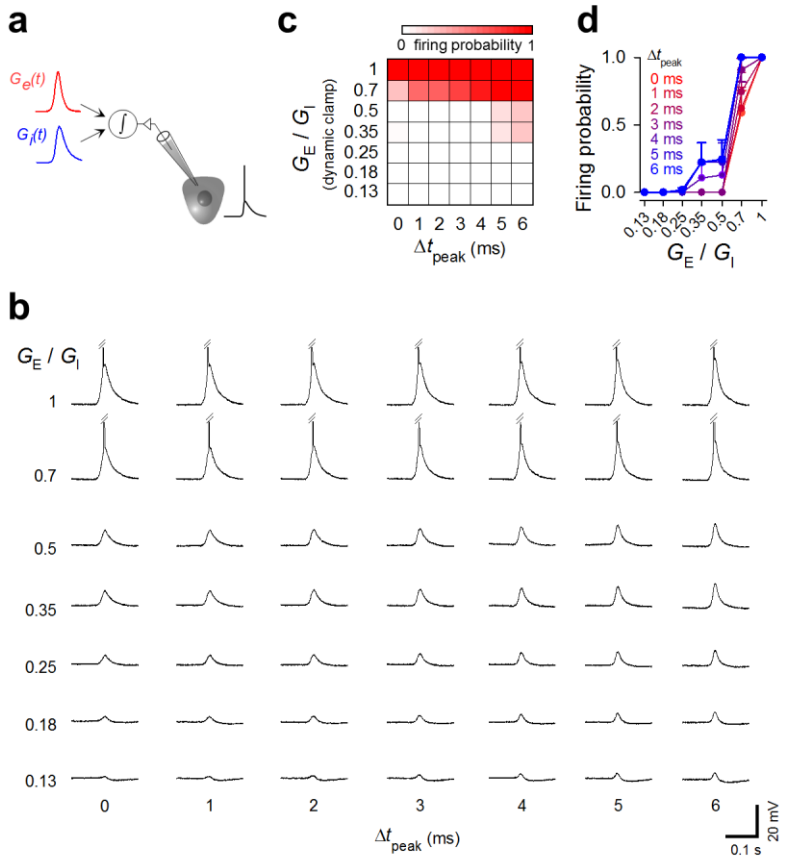

Supplementary Figure 7. Dynamic-clamp stimulation of a CA1 pyramidal cell. (a) Joint conductances of SW-relevant EPSC-like and IPSC-like waveforms were injected into a CA1 pyramidal cell under the pharmacological blockade of fast synaptic transmission. (b) Raw traces of the spike responses to the conductance injection in a representative CA1 neuron are shown with truncated spikes. The conductance peak amplitude was 0.53–4 nS for $G_e(t)$ and 4 nS for $G_i(t)$, whereas the time difference between $G_e(t)$ and $G_i(t)$ ranged from 0 to 6 ms. We tested 49 (= 7 × 7) combinations of EPSC and IPSC waveforms. (c) Pseudocolored map of the probability that CA1 pyramidal neurons fire spikes in response to dynamic-clamp conductance injection with various combinations of the EPSC-to-IPSC ratios and timings. Data were averaged from 9 neurons (20 trials each, from 5 slices in 5mice). (d) The same data shown in (c) are plotted as the means ± SD.

Nature Neuroscience: doi:10.1038/nn.3674

Data	*F*-ratio		*P*-value	
	Previous activity (dVenus +/-)	SW participation (+/-)	Previous activity (dVenus +/-)	SW participation (+/-)
SW-relevant				
EPSC size	0.012	2.19	0.46	0.07
IPSC size	0.11	0.88	0.37	0.18
E/I size	0.32	2.31	0.29	0.07
Q_E/Q_I	0.37	3.50	0.27	0.03
Δt_{peak}	1.71	0.24	0.09	0.31
Δt_{onset}	2.13	0.04	0.08	0.42
SW-irrelevant				
EPSC size	1.24	0.34	0.14	0.28
EPSC frequency	0.07	4.03	0.79	0.06
IPSC size	2.49	0.60	0.06	0.22
IPSC frequency	0.06	0.27	0.80	0.17
E/I size	0.09	0.10	0.38	0.38
E/I frequency	0.08	1.12	0.39	0.15
Q_E/Q_I	0.12	0.19	0.36	0.33

Supplementary Table 1. Statistical results of two-way ANOVA for various electrophysiological parameters. For each parameter (listed in the left-most column), datasets were separated into dVenus(+) and dVenus(–) neurons and into SW participants and nonparticipants and were tested by a two-way ANOVA. Only the *F* and *P* values for the main effect are shown because no interaction was found in any comparisons.

Nature Neuroscience: doi:10.1038/nn.3674

Supplementary Movie 1. Time-lapse confocal imaging of calcium activity from neurons. The CA1 stratum pyramidale of a hippocampal slice was loaded with Oregon Green 488 BAPTA-1, and neuronal spiking activity was monitored at 50 Hz with simultaneous LFP recording. The timings of individual SWs are indicated by flashes of a blue box.

Nature Neuroscience: doi:10.1038/nn.3674